

1    **Interpreting UniFrac with Absolute Abundance: A Conceptual and Practical Guide**

2    Augustus Pendleton<sup>1\*</sup> & Marian L. Schmidt<sup>1\*</sup>

3    <sup>1</sup>Department of Microbiology, Cornell University, 123 Wing Dr, Ithaca, NY 14850, USA

4    **Corresponding Authors:** Augustus Pendleton: arp277@cornell.edu; Marian L. Schmidt:  
5    marschmi@cornell.edu

6    **Author Contribution Statement:** Both authors contributed equally to the manuscript.

7    **Preprint servers:** This article was submitted to *bioRxiv* (doi: 10.1101/2025.07.18.665540) under  
8    a CC-BY-NC-ND 4.0 International license.

9    **Keywords:** Microbial Ecology - Beta Diversity - Absolute Abundance - Bioinformatics -  
10    UniFrac

11    **Data Availability:** All data and code used to produce the manuscript are available at  
12    [https://github.com/MarschmiLab/Pendleton\\_2025\\_Absolute\\_Unifrac\\_Paper](https://github.com/MarschmiLab/Pendleton_2025_Absolute_Unifrac_Paper), in addition to a  
13    reproducible renv environment. All packages used for analysis are listed in Table S1.

14

15    **Abstract**

16     $\beta$ -diversity is central to microbial ecology, yet commonly used metrics overlook changes in  
17    microbial load, limiting their ability to detect ecologically meaningful shifts. Popular for  
18    incorporating phylogenetic relationships, UniFrac distances currently default to relative  
19    abundance and therefore omit important variation in microbial abundances. As quantifying  
20    absolute abundance becomes more accessible, integrating this information into  $\beta$ -diversity  
21    analyses is essential. Here, we introduce *Absolute UniFrac* ( $U^A$ ), a variant of Weighted UniFrac  
22    that incorporates absolute abundances. Using simulations and a reanalysis of four 16S rRNA  
23    metabarcoding datasets (from a nuclear reactor cooling tank, the mouse gut, a freshwater lake,  
24    and the peanut rhizosphere), we demonstrate that Absolute UniFrac captures microbial load,  
25    composition, and phylogenetic relationships. While this can improve statistical power to detect  
26    ecological shifts, we also find Absolute UniFrac can be strongly correlated to differences in cell  
27    abundances alone. To balance these effects, we present the generalized extension ( $GU^A$ ) with a  
28    tunable  $\alpha$  parameter to adjust the influence of abundance and composition. Finally, we  
29    benchmark  $GU^A$  and show that although computationally slower than conventional alternatives,  
30     $GU^A$  is comparably insensitive to realistic noise in load estimates compared to conventional  
31    alternatives like Bray-Curtis dissimilarities, particularly at lower  $\alpha$ . By coupling phylogeny,  
32    composition, and microbial load, Absolute UniFrac integrates three dimensions of ecological  
33    change, better equipping microbial ecologists to quantitatively compare microbial communities.

34 **Main Text**

35 Microbial ecologists routinely compare communities using  $\beta$ -diversity metrics derived  
36 from relative abundances. Yet this approach overlooks a critical ecological dimension: microbial  
37 load. High-throughput sequencing produces compositional data, in which each taxon's  
38 abundance is constrained by all others [1]. However, quantitative profiling studies show that cell  
39 abundance, not only composition, can drive major community differences [2]. In low-biomass  
40 samples, relying on relative abundance can allow contaminants to appear biologically  
41 meaningful despite absolute counts too low for concern [3].

42 Sequencing-based microbiome studies therefore rely on relative abundance even when  
43 the hypotheses of interest implicitly concern absolute changes in biomass. This creates a  
44 mismatch between ecological framing (growth, bloom magnitude, pathogen proliferation,  
45 disturbance recovery, or colonization pressure) and the information the  $\beta$ -diversity metric  
46 encodes [4]. As a result,  $\beta$ -diversity is often treated as if it includes biomass, even when absolute  
47 abundance is either not measured at all or is measured but excluded from the calculation (as in  
48 conventional UniFrac). Many studies therefore test biomass-linked hypotheses using a metric  
49 that normalizes biomass away [4]. A conceptual correction is needed in which  $\beta$ -diversity is  
50 understood as variation along three axes: composition, phylogeny and absolute abundance.

51 Absolute microbial load measurements are now increasingly obtainable through flow  
52 cytometry, qPCR, and genomic spike-ins, allowing biomass to be quantified alongside taxonomic  
53 composition [4, 5]. These approaches improve detection of functionally relevant taxa and  
54 mitigate the compositional constraints imposed by sequencing [1, 2]. Most studies that  
55 incorporate absolute abundance counts currently rely on Bray-Curtis dissimilarity, which can  
56 capture load but does not consider phylogenetic similarity [5–7]. Unifrac distances provide the  
57 opposite strength, incorporating phylogeny but discarding absolute abundance, as they are  
58 restricted to relative abundance data by construction [8]. This leaves no phylogenetically  
59 informed  $\beta$ -diversity metric that operates on absolute counts, despite the fact that biomass is  
60 central to many ecological hypotheses.

61 To evaluate the implications of incorporating absolute abundance into phylogenetic  $\beta$ -  
62 diversity, we use both simulations and reanalysis of four 16S rRNA amplicon datasets. The  
63 simulations use a simple four-taxon community with controlled abundance shifts to directly  
64 compare both Bray-Curtis and UniFrac in their relative and absolute forms, illustrating how each  
65 metric responds when abundance, composition, or evolutionary relatedness differ. We then  
66 reanalyze four real-world datasets spanning nuclear reactor cooling water [5], the mouse gut [3],  
67 a freshwater lake [9], and rhizosphere soil [10]. These differ widely in richness, biomass range,  
68 and ecological context, allowing us to test when absolute abundance changes align with or  
69 diverge from phylogenetic turnover. Together, these simulations and reanalyses provide the  
70 empirical foundation for interpreting Absolute UniFrac relative to existing  $\beta$ -diversity measures  
71 across the three axes of ecological difference: abundance, composition, and phylogeny.

72 We also extend Absolute UniFrac as was proposed by [11] to Generalized Absolute  
73 UniFrac that incorporates a tunable ecological dimension,  $\alpha$ , and evaluate its impact across  
74 simulated and real-world datasets. As  $\alpha$  increases,  $\beta$ -diversity is increasingly correlated with  
75 differences in absolute abundance, allowing researchers to fine tune the relative weight their  
76 analyses place on microbial load versus composition.

77 **Defining Absolute UniFrac**

78 The UniFrac distance was first introduced by Lozupone & Knight (2005) and has since  
 79 become enormously popular as a measure of  $\beta$ -diversity within the field of microbial ecology  
 80 [12]. A benefit of the UniFrac distance is that it considers phylogenetic information when  
 81 estimating the distance between two communities. After first generating a phylogenetic tree  
 82 representing species (or amplicon sequence variants, “ASVs”) from all samples, the UniFrac  
 83 distance computes the fraction of branch-lengths which is *shared* between communities, relative  
 84 to the total branch length represented in the tree. UniFrac can be both unweighted, in which only  
 85 the incidence of species is considered, or weighted, wherein a branch’s contribution is weighted  
 86 by the proportional abundance of taxa on that branch [8]. The Weighted UniFrac is derived:

$$U^R = \frac{\sum_{i=1}^n b_i |p_i^a - p_i^b|}{\sum_{i=1}^n b_i (p_i^a + p_i^b)}$$

88 where the contribution of each branch length,  $b_i$ , is weighted by the difference in the relative  
 89 abundance of all species ( $p_i$ ) descended from that branch in sample  $a$  or sample  $b$ . Here, we  
 90 denote this distance as  $U^R$ , for “Relative UniFrac”. Popular packages which calculate weighted  
 91 UniFrac—including the diversity-lib QIIME plug-in and the R packages phyloseq and  
 92 GUniFrac—run this normalization by default [11, 13, 14].

93 Importantly,  $U^R$  is most sensitive to changes in abundant lineages, which can sometimes  
 94 obscure compositional differences driven by rare to moderately-abundant taxa [11]. To address  
 95 this weakness, Chen et al. (2012) introduced the generalized UniFrac distance ( $GU^R$ ), in which  
 96 the impact of abundant lineages can be mitigated by decreasing the parameter  $\alpha$ :

$$GU^R = \frac{\sum_{i=1}^n b_i (p_i^a + p_i^b)^\alpha \left| \frac{p_i^a - p_i^b}{p_i^a + p_i^b} \right|}{\sum_{i=1}^n b_i (p_i^a + p_i^b)^\alpha}$$

98 where  $\alpha$  ranges from 0 (close to Unweighted UniFrac) up to 1 (identical to  $U^R$ , above). However,  
 99 if one wishes to use absolute abundances, both  $U^R$  and  $GU^R$  can be derived without normalizing  
 100 to proportions:

$$U^A = \frac{\sum_{i=1}^n b_i |c_i^a - c_i^b|}{\sum_{i=1}^n b_i (c_i^a + c_i^b)} \quad GU^A = \frac{\sum_{i=1}^n b_i (c_i^a + c_i^b)^\alpha \left| \frac{c_i^a - c_i^b}{c_i^a + c_i^b} \right|}{\sum_{i=1}^n b_i (c_i^a + c_i^b)^\alpha}$$

102 Where  $c_i^a$  and  $c_i^b$  denote for the absolute counts of species descending from branch  $b_i$  in  
 103 communities  $a$  and  $b$ , respectively. We refer to these distances as *Absolute UniFrac* ( $U^A$ ) and  
 104 *Generalized Absolute UniFrac* ( $GU^A$ ). Although substituting absolute for relative abundances is  
 105 mathematically straightforward, we found no prior work that examines UniFrac in the context of  
 106 absolute abundance, either conceptually or in application. Incorporating absolute abundances  
 107 introduces a third axis of ecological variation: beyond differences in composition and  
 108 phylogenetic similarity,  $U^A$  also captures divergence in microbial load. This makes interpretation  
 109 of  $U^A$  nontrivial, particularly in complex microbiomes.

110 **Demonstrating  $\beta$ -diversity metrics’ behavior with a simple simulation**

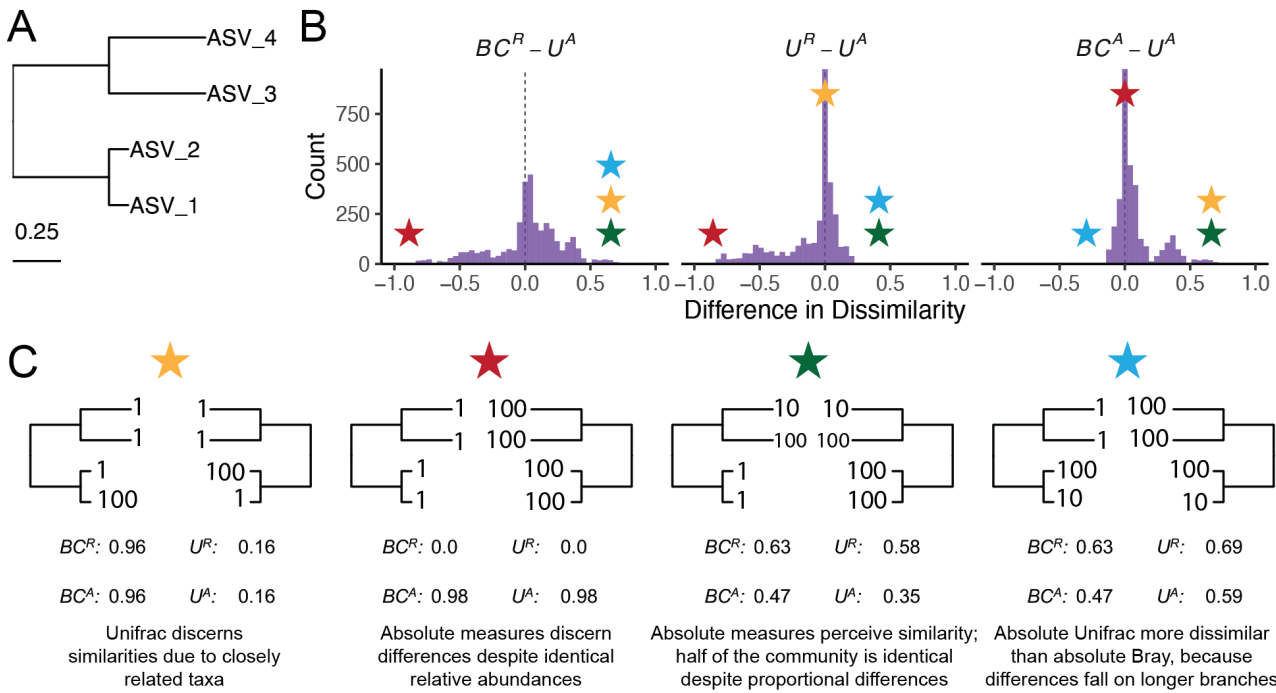
To clarify how  $U^A$  behaves relative to existing  $\beta$ -diversity metrics, we first constructed a simple four-taxon simulated community arranged in a small phylogeny (Fig. 1A). By varying the absolute abundance of each ASV (1, 10, or 100), we generated 81 samples and 3,240 pairwise comparisons. For each pair, we computed four dissimilarity metrics: Bray-Curtis with relative abundance ( $BC^R$ ), Bray-Curtis with absolute abundance ( $BC^A$ ), Weighted UniFrac with relative abundance ( $U^R$ ), and Weighted UniFrac with absolute abundance ( $U^A$ ). These comparisons help to illustrate how each axis of ecological difference—abundance, composition, and phylogeny—is expressed by the different metrics.

$U^A$  does not consistently yield higher or lower distances compared to other metrics, but instead varies depending on how abundance and phylogeny intersect (Fig. 1B). In the improbable scenario that all branch lengths are equal,  $U^A$  is always less than or equal to  $BC^A$  (Fig. S1). These comparisons emphasize that once branch lengths differ, incorporating phylogeny and absolute abundance alters the structure of the distance space. The direction and magnitude of that change depend on which branches carry the abundance shifts.  $U^A$  is also usually smaller than  $BC^A$  and is more strongly correlated with  $BC^A$  (Pearson's  $r = 0.82$ ,  $p < 0.0001$ ) than with  $BC^R$  ( $r = 0.41$ ) and  $U^R$  ( $r = 0.55$ ).

To better understand how these metrics diverge, we examined individual sample pairs (Fig. 1C). Scenario 1 (gold star) illustrates the classic advantage of UniFrac: ASV\_1 and ASV\_2 are phylogenetically close, so  $U^R$  and  $U^A$  discern greater similarity between samples than  $BC^R$  and  $BC^A$ , which ignore phylogenetic structure. Scenario 2 (red star) highlights a limitation of relative metrics: two samples with identical relative composition but a 100-fold difference in biomass appear identical to  $BC^R$  and  $U^R$ , but not to their absolute counterparts. In Scenario 3 (green star), incorporating absolute abundance decreases dissimilarity.  $BC^A$  and  $U^A$  are lower than their relative counterparts because half the community is identical in absolute abundance, even though their proportions differ. In contrast, Scenario 4 (blue star) shows that  $U^A$  can exceed  $BC^A$  when abundance differences occur on long branches, amplifying phylogenetic dissimilarity.

These scenarios demonstrate that  $U^A$  integrates variation along three ecologically relevant axes: composition, phylogenetic similarity, and microbial load, rather than isolating any single dimension. Because a given  $U^A$  value can reflect multiple drivers of community change, interpreting it requires downstream analyses to disentangle the relative contributions of these three axes. To evaluate how this plays out in real systems we next reanalyzed four previously published datasets spanning diverse microbial environments.

143  
144  
145

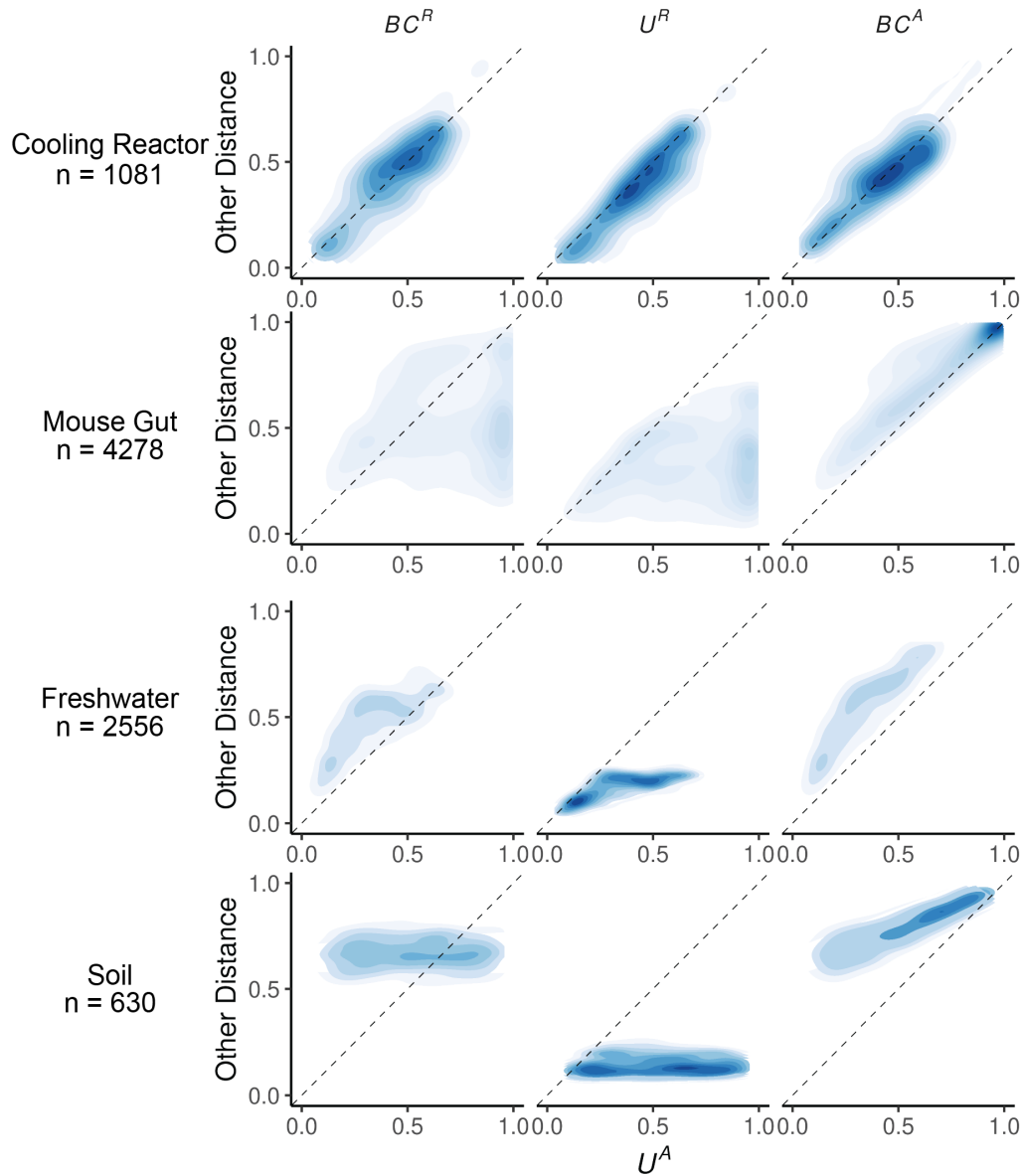


146 *Figure 1. Simulated communities reveal how absolute abundance affects phylogenetic and non-phylogenetic  $\beta$ -*  
147 *diversity measures.* (A) We constructed a simple four-ASV community with a known phylogeny and generated all  
148 permutations of each ASV having an absolute abundance of 1, 10, or 100, resulting in 81 unique communities and  
149 3,240 pairwise comparisons. (B) Distributions of pairwise differences between weighted UniFrac using absolute  
150 abundance ( $U^A$ ) and three other metrics: Bray-Curtis using relative abundance ( $BC^R$ ), weighted UniFrac using  
151 relative abundance ( $UR$ ), and Bray-Curtis using absolute abundance ( $BC^A$ ). (C) Illustrative sample pairs demonstrate  
152 how absolute abundances and phylogenetic structure interact to increase or decrease dissimilarity across metrics.  
153 Stars indicate where each scenario falls within the distributions shown in panel B. Actual values for each metric are  
154 displayed beneath each scenario.

## 155 Application of Absolute UniFrac to Four Real-World Microbiome Datasets

156 To illustrate the sensitivity of  $U^A$  to both variation in composition and absolute  
157 abundance, we re-analyzed four previously published datasets from diverse microbial systems.  
158 These datasets included: (i) nuclear reactor cooling water sampled across three reactor cycle  
159 phases [5]; (ii) the mouse gut sampled across multiple regions and between two diets [3]; (iii)  
160 depth-stratified freshwater communities sampled across two months [9]; and (iv) peanut  
161 rhizospheres under two crop rotation schemes (conventional rotation (CR) vs. sod-based rotation  
162 (SBR)), plant maturities, and irrigation treatments [10]. Absolute abundance was quantified by  
163 flow cytometry for the cooling water and freshwater datasets, droplet digital PCR for the mouse  
164 gut, and by qPCR for the rhizosphere dataset. Together these span a wide range of richness—from  
165 215 ASVs in the cooling water to 24,000 ASVs in the soil—and microbial load—from as low as  
166  $4 \times 10^5$  cells/ml (cooling water) up to  $2 \times 10^{12}$  16S rRNA copies/gram (mouse gut). Additional

167 details of the re-analysis workflow, including ASV generation and phylogenetic inference, are  
168 provided in the Supporting Methods.



169 *Figure 2. Absolute UniFrac ( $U^A$ ) compared with other  $\beta$ -diversity metrics across four real microbial datasets.* Each  
170 panel shows pairwise sample distances for  $U^A$  (x-axis) against another metric (y-axis): Bray-Curtis using relative  
171 abundance ( $BC^R$ , first column), weighted UniFrac using relative abundances ( $U^R$ , second column), and Bray-curtis  
172 using absolute abundances ( $BC^A$ , third column). Contours indicate the relative density of pairwise comparisons (n  
173 shown for each dataset, left), with darker shading corresponding to more observations. The dashed line marks the  
174 1:1 relationship. Points above the line indicate cases where  $U^A$  is smaller than the comparator metric, while points  
175 below the line indicate cases where  $U^A$  is larger.

176 We first calculated four  $\beta$ -diversity metrics for all sample pairs in each dataset and  
177 compared them to  $U^A$  (Fig. 2). The degree of concordance between  $U^A$  and other metrics was  
178 highly context dependent. In the cooling water dataset,  $U^A$  closely tracked all three alternatives,  
179 whereas in the remaining systems it diverged substantially.  $U^A$  also spanned a similar or wider

180 range of distances than the other metrics. For example, in the soil dataset  $BC^R$  and  $U^R$  occupied a  
181 narrow range relative to the broad separation observed under  $U^A$ .

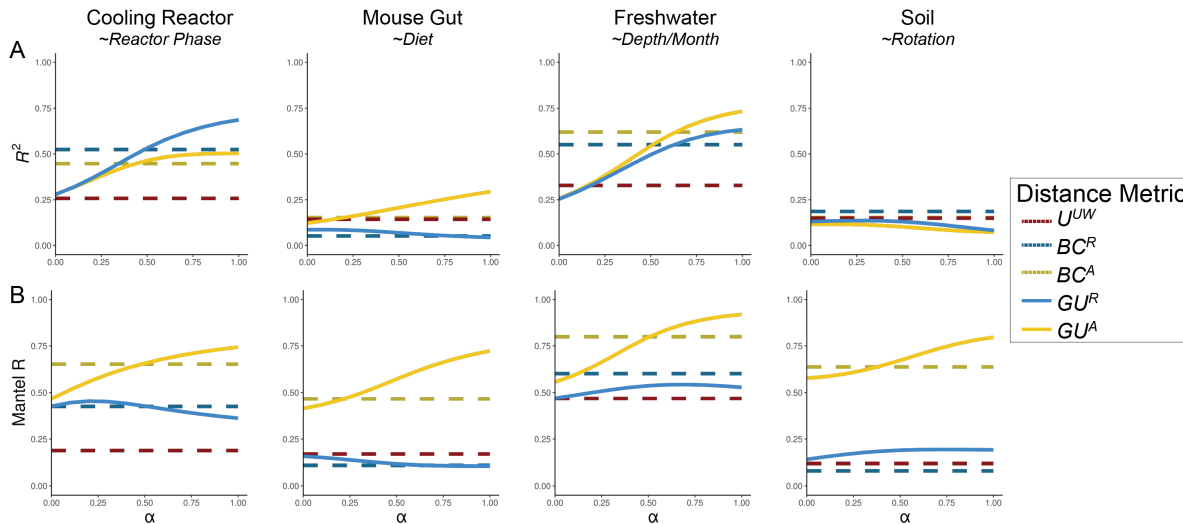
182  $U^A$  generally reported distances that were similar to or greater than  $U^R$ , consistent with  
183 the simulations shown in Fig. 1B. This reflects the ability of  $U^A$  to discern dissimilarity due to  
184 differences in microbial load, even when community composition is conserved. In contrast,  $U^A$   
185 yielded distances that were similar to or lower than  $BC^A$ , again matching the simulated behavior  
186 in Fig 1B. In these cases, phylogenetic proximity between abundant, closely-related ASVs leads  
187  $U^A$  to register greater similarity than  $BC^A$ .

188 Given these differences, we next quantified how well each metric discriminates among  
189 categorical sample groups. For each dataset, we ran PERMANOVAs to measure the proportion  
190 of variance ( $R^2$ ) and statistical power (*pseudo-F*, *p*-value) attributable to group structure, using  
191 groupings that were determined to be significant in the original publications. To evaluate how  
192 strongly absolute abundance contributed to this discrimination, we also calculated  $GU^A$  across a  
193 range of  $\alpha$  values. The resulting  $R^2$  values are displayed in Fig. 3A, with the corresponding  
194 *pseudo-F* statistics and *p*-values provided in Fig. S2.

195 As in Fig. 2, the performance of each metric was strongly context dependent (Fig. 3A). In the  
196 mouse gut and freshwater datasets, absolute-abundance-aware metrics ( $BC^A$  and  $GU^A$ ) explained  
197 the greatest proportion of variance ( $R^2$ ), and  $R^2$  generally increasing as  $\alpha$  increased. In contrast,  
198 relative metrics captured more variation in the cooling water dataset (again at higher  $\alpha$ ), and all  
199 metrics explained comparably little variance in the soil dataset. Taken at face value, these trends  
200 might suggest that higher  $\alpha$  values typically improve group differentiation.

201 However, this comes with a major caveat: at high  $\alpha$  values,  $GU^A$  becomes strongly  
202 correlated with total cell count alone (Fig. 3B). Mantel tests confirmed that absolute-abundance  
203 metrics are far more sensitive to differences in microbial load than their relative counterparts.  
204 This behavior is intuitive, and to some extent desirable, because these metrics are designed to  
205 detect changes in microbial load even when composition remains constant. Yet at  $\alpha = 1$ ,  $U^A$   
206 approaches a proxy for sample absolute abundance itself. In ordination space (Fig. S3), this can  
207 cause Axis 1 to correlate with absolute abundance and in some cases (freshwater and soil)  
208 produces strong horseshoe effects [15], potentially distorting ecological interpretation.

209



210  
 211 *Figure 3. Discriminatory performance of  $U^A$  and related metrics across four microbial systems.* (A) PERMANOVAs  
 212 were used to quantify the percent variance ( $R^2$ ) explained by predefined categorical groups (shown in italics beneath  
 213 each dataset name), with 1,000 permutations. Metrics were evaluated across five metrics and, where applicable,  
 214 across eleven  $\alpha$  values (0-1 in 0.1 increments). For consistency with the original studies, only samples from Reactor  
 215 cycle 1 were used for the cooling-water dataset, only stool samples for the mouse gut dataset, and only mature  
 216 rhizosphere samples for the dataset. (B) Mantel correlation (R) between each distance metric and the pairwise  
 217 differences in absolute abundance (cell counts or 16S copy number), illustrating the degree to which each metric is  
 218 driven by biomass differences.

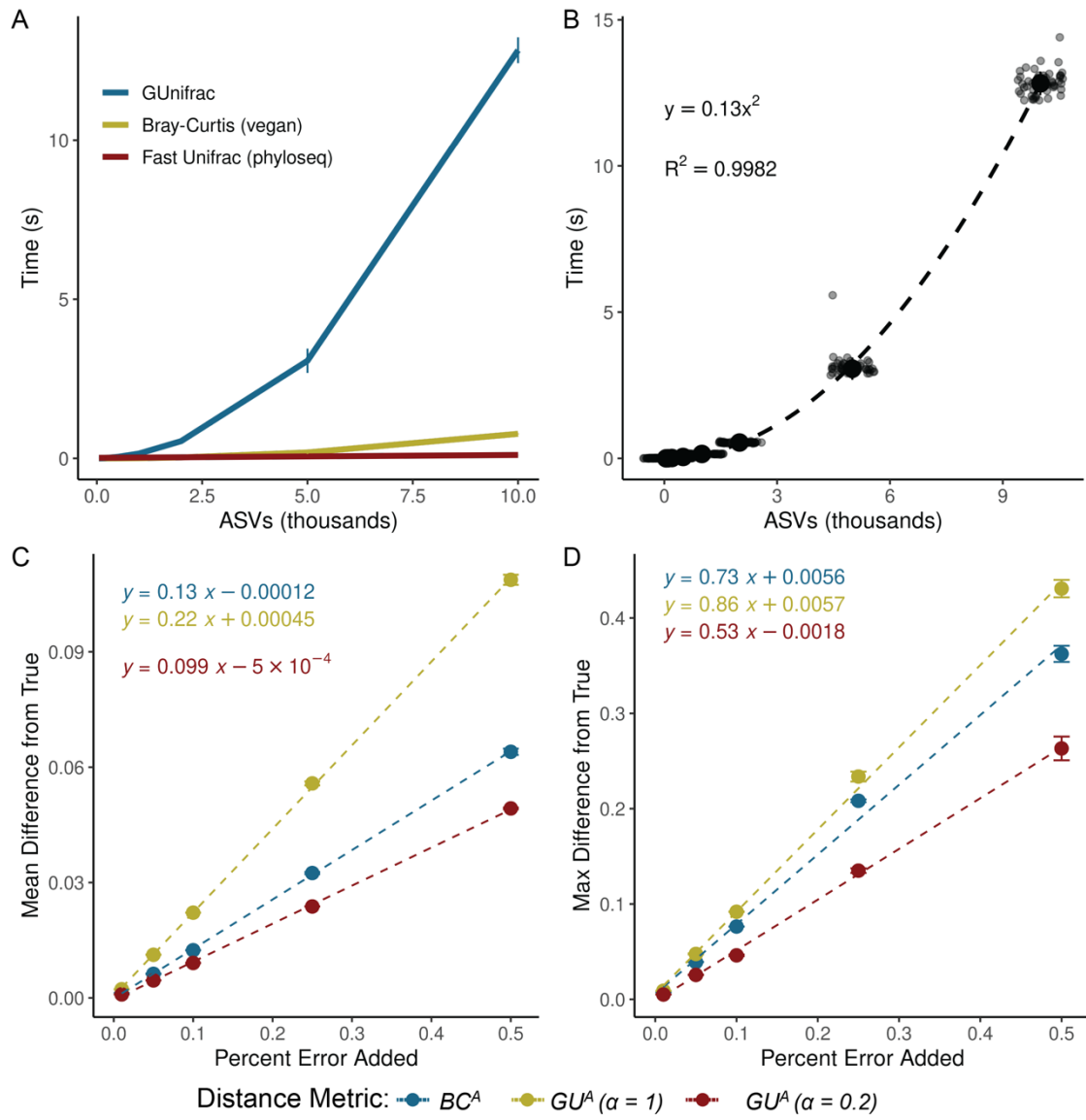
219 We recommend calibrating  $\alpha$  based on research goals, modulating this effect by using  
 220  $GU^A$  across a range of  $\alpha$  rather than relying on  $U^A$  ( $\alpha = 1$ ). Researchers should consider how  
 221 much emphasis they want their dissimilarity metric to place on microbial load (Box 1). When  
 222 biomass differences are central to the hypothesis being tested (for example, detecting  
 223 cyanobacterial blooms), high  $\alpha$  are recommended. In contrast, if microbial load is irrelevant or  
 224 independent of the hypothesis in question, low  $\alpha$  (or  $U^R$ ) may be preferred; for example in the  
 225 soil dataset, fine-scale differences in composition may be obscured by random variation in  
 226 microbial load.

227 In many systems, microbial biomass is one piece of the story, likely correlated to other  
 228 variables being tested. If the importance of microbial load in the system is unknown, one  
 229 potential approach is to calculate correlations as demonstrated in Fig. 3B and select an  $\alpha$  prior to  
 230 any ordinations or statistical testing. Again, absolute metrics are expected to correlate to  
 231 differences in cell count, as we hope absolute abundance measures incorporate differences in cell  
 232 counts, especially when microbial load is relevant to the hypotheses being tested. Correlations to  
 233 cell count in  $BC^A$ , an accepted approach in the literature, ranged from ~0.5 up to ~0.8. As a  
 234 general recommendation from these analyses, we recommend  $\alpha$  values in an intermediate range  
 235 from 0.1 up to 0.6.

### 236 Computational and Methodological Considerations

237 Applying  $GU^A$  in practice raises several considerations related to sequencing depth,  
 238 richness, and computational cost. Both Bray-Curtis and UniFrac can be sensitive to sequencing  
 239 depth because richness varies with read count [16–18]. Methods to address these concerns,  
 240 including rarefaction, remain debated and are challenging to benchmark rigorously [19]. We do  
 241 not evaluate the sensitivity of  $U^A$  or  $GU^A$  to different rarefaction strategies here, but we do

241 provide a workflow and code for how we incorporated rarefaction into our own analyses (Box 2  
 242 and available code). This approach minimizes sequencing-depth biases while preserving  
 243 abundance scaling for downstream  $\beta$ -diversity analysis.



244  
 245 *Figure 4.  $GU^A$  requires more computational time but remains resilient to quantification error.* (A) Runtime for  $GU^A$   
 246 (GUniFrac package),  $U^R$  (FastUniFrac in the phyloseq package) and  $BC^A$  (vegan package) was benchmarked across  
 247 50 iterations on a sub-sampled soil dataset (mature samples only) [10], using increasing ASV richness (50, 100, 200,  
 248 500, 1,000, 2,000, 5,000, 10,000), with 10 samples and one  $\alpha$  value per run (unweighted UniFrac is also calculated  
 249 by default). Error bars represent standard deviation. (B) Quadratic relationship between  $GU^A$  computation time and  
 250 ASV richness. Large center point represents median across 50 iterations, error bars (standard deviation) are too  
 251 small to be seen. (C-D) Sensitivity of  $GU^A$  ( $\alpha = 1$  and 0.2) and  $BC^A$  to measurement error was evaluated by adding  
 252 random variation ( $\pm 1\%$  to  $\pm 50\%$ ; Supporting Methods) to 16S copy number estimates in stool samples from the  
 253 mouse gut dataset [3]. For each error level, 50 replicate matrices were generated and compared to the original  
 254 values. Panels reflect the (C) mean difference and (D) max difference between the error-added metrics compared to  
 255 the originals. Error bars represent the standard deviation of the average mean and max difference across 50  
 256 iterations.

257         $GU^A$  is slower to compute than both  $BC^A$  and  $U^R$  because it must traverse the phylogenetic  
258 tree to calculate branch lengths for each iteration. Computational time of  $GU^A$  increases  
259 quadratically with ASV number and is 10-20 times slower, though up to 50 times slower, than  
260  $BC^A$  (Fig. 4A-B). The number of samples or  $\alpha$  values, however, have relatively little effect on  
261 runtime (Fig. S4). For a dataset of 24,000 ASVs, computing on a single CPU is still reasonable  
262 (1.4 minutes), but repeated rarefaction increases runtime substantially because branch lengths are  
263 redundantly calculated with each iteration. Allowing branch-length objects to be cached or  
264 incorporated directly into the GUnifrac workflow would considerably improve computational  
265 efficiency.

266        We also evaluated the sensitivity of  $GU^A$  to measurement error in absolute abundance due  
267 to uncertainty arising from the quantification of cell number of 16S copy number. To assess the  
268 sensitivity of  $GU^A$  and  $BC^A$  to measurement error, we added random error to the 16S copy  
269 number measurements from the mouse gut dataset, limiting our analyses to the stool samples  
270 where copy numbers varied by an order of magnitude. Across 50 iterations, each copy number  
271 could randomly vary by a given percentage of error in either direction. We re-calculated  $\beta$ -  
272 diversity ( $BC^A$  and  $GU^A$  at  $\alpha = 1$  and  $\alpha = 0.2$ ) and compared these measurements to the original  
273 dataset.

274        Introducing random variation into measured 16S copy number altered  $GU^A$  values only  
275 modestly, and the effect was proportional to the magnitude of the added noise (Fig. 4C-D). At  $\alpha$   
276 = 1, each 1% of quantification error introduced an average difference of 0.0022 in GUA; at  $\alpha =$   
277 0.2, GUA was even less sensitive. Thus, moderate  $\alpha$  values provide a balance between  
278 interpretability and robustness to noise in absolute quantification. The max deviation from true  
279 that added error could inflict on a given metric was also proportional (and always less) than the  
280 magnitude of the error itself (Fig. 4D). A more rigorous approach to assessing error propagation  
281 within these metrics, including mathematical proofs of the relationships estimated above, is  
282 outside the scope of this paper but would be helpful.

### 283 **Ecological Interpretation and conceptual significance**

284        Absolute UniFrac reframes the interpretation of  $\beta$ -diversity by making biomass an explicit  
285 ecological axis rather than an unmeasured or normalized-away quantity. Conventional UniFrac  
286 capture composition and shared evolutionary history, but implicitly invites interpretation as if it  
287 also encodes differences on microbial load. By incorporating absolute abundance directly,  
288 Absolute UniFrac helps to resolve this mismatch and restores alignment between ecological  
289 hypotheses and the quantities represented in the metric. In this view,  $\beta$ -diversity becomes a three-  
290 axis ecological measure, incorporating composition, phylogeny and biomass, rather than a two-  
291 axis approximation. That said, the additional dimension of microbial load also increases the  
292 complexity of applying and interpreting this metric.

293        There are many cases where the incorporation of absolute abundance allows microbial  
294 ecologists to assess more realistic, ecologically-relevant differences in microbial communities,  
295 especially when microbial load is mechanistically central. Outside of the datasets re-analyzed  
296 here [3, 5, 9, 10]; the temporal development of the infant gut microbiome involves both a rise in  
297 absolute abundance and compositional changes [6]; bacteriophage predation in wastewater  
298 bioreactors can be understood only when microbial load is considered [20]; and antibiotic-driven  
299 declines in specific swine gut taxa were missed using relative abundance approaches [21]. As  $\beta$ -

300 diversity metrics (and UniFrac specifically) remain central to microbial ecology, these findings  
301 highlight how interpretation changes once biomass is incorporated. Broader adoption of absolute  
302 abundance profiling will also depend on data availability. Few studies currently make absolute  
303 quantification data publicly accessible, underscoring the need to deposit absolute measurements  
304 alongside sequencing reads for reproducibility, ideally as metadata within SRA submissions.

305 While demonstrated here with 16S rRNA data, the approach should extend to other marker  
306 genes or (meta)genomic features, provided absolute abundance estimates are available. In this  
307 sense,  $GU^A$  offers a more ecologically grounded view of lineage turnover by jointly reflecting  
308 variation in biomass and phylogenetic structure.

309 No single metric (or  $\alpha$  in  $GU^A$ ), however, is universally “best”. Each  $\beta$ -diversity metric  
310 emphasizes a different dimension of community change. Researchers should therefore select  
311 metrics based on the ecological quantity that is hypothesized to matter most. Here, we  
312 demonstrate not that  $GU^A$  outperforms other measures, but that it faithfully incorporates the three  
313 axes of variation it was designed to incorporate: composition, phylogenetic similarity, and  
314 absolute abundance (Fig. 1 and Fig. 2). As with any  $\beta$ -diversity analysis, interpretation requires  
315 matching the metric to the ecological question at hand, and exploring sensitivity across different  
316 metrics where appropriate [22]. By providing demonstrations and code for the application and  
317 interpretation of  $U^A/GU^A$ , we hope to encourage the use of these metrics as a tool of microbial  
318 ecology.

### 319 Conclusion

320 By explicitly incorporating absolute abundance, Absolute UniFrac shifts phylogenetic  $\beta$ -  
321 diversity from a two-axis approximation to a three-axis ecological measure. This reframing  
322 connects the metric to the underlying biological questions that motivate many microbiome  
323 studies. As methods for quantifying microbial load continue to expand, the ability to interpret  $\beta$ -  
324 diversity in a biomass-aware framework will become increasingly important for distinguishing  
325 true ecological turnover from proportional change alone. In this way, Absolute UniFrac is not  
326 simply an alternative distance metric but a tool for aligning statistical representation with  
327 ecological mechanism.

328

329

330 **Box 1:  $\beta$ -diversity metrics should reflect the hypothesis being tested**

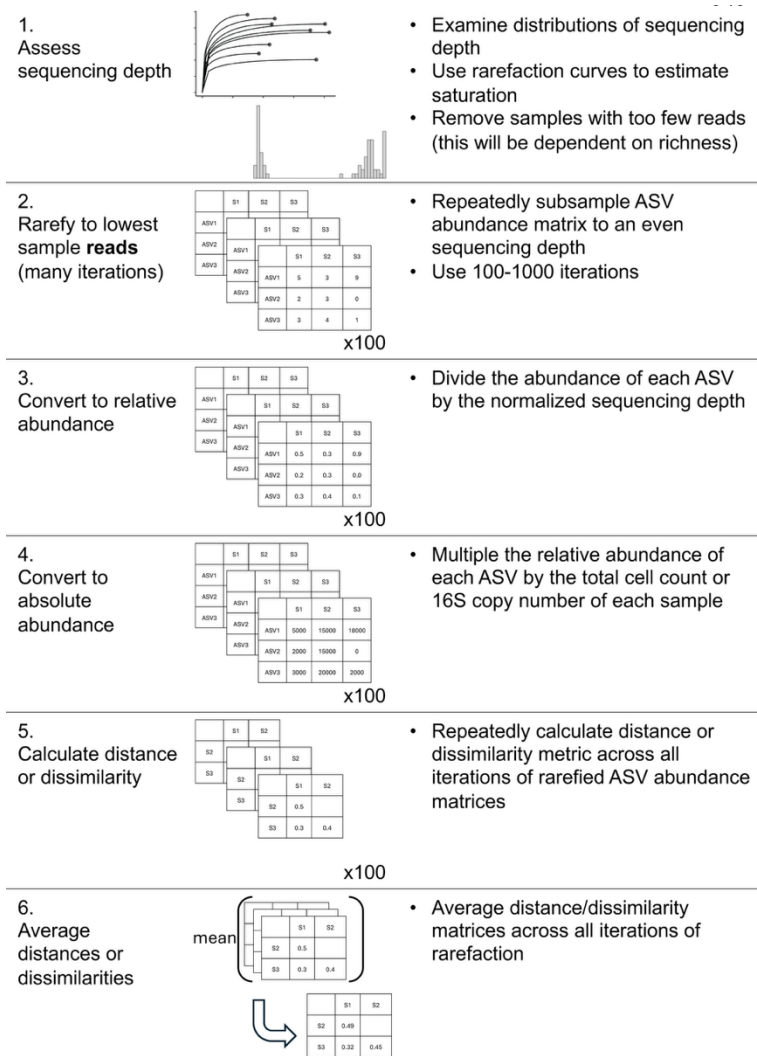
331 Absolute UniFrac is most informative when variation in microbial load is expected to carry  
 332 ecological meaning rather than being a nuisance variable. The choice of  $\alpha$  determines how  
 333 strongly abundance differences influence the metric, and should therefore be selected based on  
 334 the hypothesis, not by convention. In settings where biomass is central to the mechanism under  
 335 study, higher  $\alpha$  values appropriately foreground that signal, whereas in cases where load  
 336 variation is incidental or confounding, lower  $\alpha$  values maintain interpretability. Framing  $\alpha$  as a  
 337 hypothesis-driven choice repositions  $\beta$ -diversity from a default normalization step to an explicit  
 338 ecological decision.

				Metric to Use	Hypothetical Example
Treat closely related lineages as similar?	Yes	How relevant is microbial load?	Central to hypothesis	$GU^A, \alpha > 0.5$	Cyanobacterial bloom, pathogen proliferation
			Relevant, but associated with other variables of interest	$GU^A, 0.1 < \alpha < 0.5$	Compositional shifts in response to nutrient addition
			Irrelevant	Dominant	$GU^R, \alpha > 0.5$
				Rare	$GU^R, \alpha < 0.5$
	No	Microbial load relevant?	Unknown	$GU^A$ at multiple $\alpha$	Random variation in microbial load obscured compositional shifts in soil communities
			Yes	$BC^A$	Strain turnover and proliferation in the infant gut
			No	$BC^R$	Temporal succession in chemostat

339

340

## 342 Box 2: Rarefaction workflow for incorporating absolute abundance



While we refrain from an in-depth analysis of rarefaction approaches, here we present our workflow for incorporating rarefaction alongside absolute abundance. First, samples were assessed for anomalously low read counts and discarded (sequencing blanks and controls were also removed). For rarefaction, each sample in ASV table was subsampled to equal *sequencing depth* (# of reads) across 100 iterations, creating 100 rarefied ASV tables. These tables were then converted to relative abundance by dividing each ASV's count by the equal sequencing depth (rounding was not performed). Then, each ASV's absolute abundance within a given sample was calculated by multiplying its relative abundance by that sample's total cell count or 16S copy number. Methods to predict genomic 16S copy number for a given ASV were not used

368

369 [23]. Each distance/dissimilarity metric was then calculated across all 100 absolute-normalized  
 370 ASV tables. The final distance/dissimilarity matrix was calculated by averaging all 100 iterations  
 371 of each distance/dissimilarity calculation. Of note for future users: pruning the phylogenetic tree  
 372 after rarefaction for each iteration is not necessary – ASVs removed from the dataset do not  
 373 contribute nor change the calculated UniFrac distances.

374

- 375
- 376
- 377 **References**
- 378 1. Gloor GB et al. Microbiome Datasets Are Compositional: And This Is Not Optional. *Front*  
379 *Microbiol* 2017;8:2224. <https://doi.org/10.3389/fmicb.2017.02224>
- 380 2. Vandepitte D et al. Stool consistency is strongly associated with gut microbiota richness  
381 and composition, enterotypes and bacterial growth rates. *Gut* 2016;65:57–62.  
382 <https://doi.org/10.1136/gutjnl-2015-309618>
- 383 3. Barlow JT, Bogatyrev SR, Ismagilov RF. A quantitative sequencing framework for absolute  
384 abundance measurements of mucosal and luminal microbial communities. *Nat Commun*  
385 2020;11:2590. <https://doi.org/10.1038/s41467-020-16224-6>
- 386 4. Wang X et al. Current Applications of Absolute Bacterial Quantification in Microbiome  
387 Studies and Decision-Making Regarding Different Biological Questions. *Microorganisms*  
388 2021;9:1797. <https://doi.org/10.3390/microorganisms9091797>
- 389 5. Props R et al. Absolute quantification of microbial taxon abundances. *ISME J* 2017;11:584–  
390 587. <https://doi.org/10.1038/ismej.2016.117>
- 391 6. Rao C et al. Multi-kingdom ecological drivers of microbiota assembly in preterm infants.  
392 *Nature* 2021;591:633–638. <https://doi.org/10.1038/s41586-021-03241-8>
- 393 7. Bray JR, Curtis JT. An Ordination of the Upland Forest Communities of Southern  
394 Wisconsin. *Ecological Monographs* 1957;27:326–349. <https://doi.org/10.2307/1942268>
- 395 8. Lozupone CA et al. Quantitative and Qualitative  $\beta$  Diversity Measures Lead to Different  
396 Insights into Factors That Structure Microbial Communities. *Applied and Environmental*  
397 *Microbiology* 2007;73:1576–1585. <https://doi.org/10.1128/AEM.01996-06>

- 398 9. Pendleton A, Wells M, Schmidt ML. Upwelling periodically disturbs the ecological  
399 assembly of microbial communities in the Laurentian Great Lakes. 2025. bioRxiv, 2025. ,  
400 2025.01.17.633667
- 401 10. Zhang K et al. Absolute microbiome profiling highlights the links among microbial  
402 stability, soil health, and crop productivity under long-term sod-based rotation. *Biol Fertil  
403 Soils* 2022;58:883–901. <https://doi.org/10.1007/s00374-022-01675-4>
- 404 11. Chen J et al. Associating microbiome composition with environmental covariates using  
405 generalized UniFrac distances. *Bioinformatics* 2012;28:2106–2113.  
406 <https://doi.org/10.1093/bioinformatics/bts342>
- 407 12. Lozupone C, Knight R. UniFrac: a New Phylogenetic Method for Comparing Microbial  
408 Communities. *Applied and Environmental Microbiology* 2005;71:8228–8235.  
409 <https://doi.org/10.1128/AEM.71.12.8228-8235.2005>
- 410 13. McMurdie PJ, Holmes S. phyloseq: An R package for reproducible interactive analysis and  
411 graphics of microbiome census data. *PLoS ONE* 2013;8:e61217.
- 412 14. Bolyen E et al. Reproducible, interactive, scalable and extensible microbiome data science  
413 using QIIME 2. *Nat Biotechnol* 2019;37:852–857. [https://doi.org/10.1038/s41587-019-0209-9](https://doi.org/10.1038/s41587-019-<br/>414 0209-9)
- 415 15. Morton JT et al. Uncovering the Horseshoe Effect in Microbial Analyses. *mSystems*  
416 2017;2:10.1128/msystems.00166-16. <https://doi.org/10.1128/msystems.00166-16>
- 417 16. Schloss PD. Evaluating different approaches that test whether microbial communities have  
418 the same structure. *The ISME Journal* 2008;2:265–275.  
419 <https://doi.org/10.1038/ismej.2008.5>

- 420 17. Fukuyama J et al. Comparisons of distance methods for combining covariates and  
421 abundances in microbiome studies. *Biocomputing 2012*. WORLD SCIENTIFIC, 2011,  
422 213–224.
- 423 18. McMurdie PJ, Holmes S. Waste Not, Want Not: Why Rarefying Microbiome Data Is  
424 Inadmissible. *PLOS Computational Biology* 2014;10:e1003531.  
425 <https://doi.org/10.1371/journal.pcbi.1003531>
- 426 19. Schloss PD. Waste not, want not: revisiting the analysis that called into question the  
427 practice of rarefaction. *mSphere* 2023;9:e00355-23. <https://doi.org/10.1128/mSphere.00355-23>
- 429 20. Shapiro OH, Kushmaro A, Brenner A. Bacteriophage predation regulates microbial  
430 abundance and diversity in a full-scale bioreactor treating industrial wastewater. *The ISME  
431 Journal* 2010;4:327–336. <https://doi.org/10.1038/ismej.2009.118>
- 432 21. Wagner S et al. Absolute abundance calculation enhances the significance of microbiome  
433 data in antibiotic treatment studies. *Front Microbiol* 2025;16.  
434 <https://doi.org/10.3389/fmicb.2025.1481197>
- 435 22. Kers JG, Saccenti E. The Power of Microbiome Studies: Some Considerations on Which  
436 Alpha and Beta Metrics to Use and How to Report Results. *Front Microbiol* 2022;12.  
437 <https://doi.org/10.3389/fmicb.2021.796025>
- 438 23. Douglas GM et al. PICRUSt2 for prediction of metagenome functions. *Nat Biotechnol*  
439 2020;38:685–688. <https://doi.org/10.1038/s41587-020-0548-6>
- 440